LBNL-6097E

ERNEST ORLANDO LAWRENCE
BERKELEY NATIONAL LABORATORY

Effect of the shutdown of a large coal-fired power plant on ambient mercury species

Yungang Wang[1], Jiaoyan Huang[2,a], Philip K. Hopke[3,*], Oliver V. Rattigan[4], David C. Chalupa[5], Mark J. Utell[5],Thomas M. Holsen[2,3]

[1]Environmental Energy Technologies Division
Lawrence Berkeley National Laboratory
Berkeley, CA 94720, USA

[2] Department of Civil and Environmental Engineering
Clarkson University, Potsdam, NY 13699, USA

[3]Center for Air Resource Engineering and Science
Clarkson University, Potsdam, NY 13699, USA

[4]Division of Air Resources
New York State Department of Environmental Conservation
Albany, NY 12233, USA

[5]Department of Environmental Medicine
University of Rochester Medical Center, Rochester, NY 14642, USA

January 2013

This work was supported by the New York State Energy Research and Development Authority (NYSERDA) through Contracts 8650 and 10604; the United States Environmental Protection Agency (US EPA) through Science to Achieve Results (STAR) grant RD83241501; a Syracuse Center of Excellence Collaborative Activities for Research and Technology Innovation (CARTI) project award, which is supported by a grant from the US EPA (Award No: X-83232501-0); the Electric Power Research Institute under Agreement W06325; the US EPA Atmospheric Clean Air Markets Division and NADP Hg Monitoring Network (EP08H000271) through the U.S. Department of Energy under contract DE-AC02-05CH11231.

Disclaimer

This document was prepared as an account of work sponsored by the United States Government. While this document is believed to contain correct information, neither the United States Government nor any agency thereof, nor The Regents of the University of California, nor any of their employees, makes any warranty, express or implied, or assumes any legal responsibility for the accuracy, completeness, or usefulness of any information, apparatus, product, or process disclosed, or represents that its use would not infringe privately owned rights. Reference herein to any specific commercial product, process, or service by its trade name, trademark, manufacturer, or otherwise, does not necessarily constitute or imply its endorsement, recommendation, or favoring by the United States Government or any agency thereof, or The Regents of the University of California. The views and opinions of authors expressed herein do not necessarily state or reflect those of the United States Government or any agency thereof, or The Regents of the University of California.

Ernest Orlando Lawrence Berkeley National Laboratory is an equal opportunity employer.

Effect of the shutdown of a large coal-fired power plant on ambient mercury species

Yungang Wang[1], Jiaoyan Huang[2,a], Philip K. Hopke[3,*], Oliver V. Rattigan[4], David C. Chalupa[5], Mark J. Utell[5],Thomas M. Holsen[2,3]

[1]Environmental Energy Technologies Division, Lawrence Berkeley National Laboratory, Berkeley, CA 94720, USA

[2] Department of Civil and Environmental Engineering, Clarkson University, Potsdam, NY 13699, USA

[3]Center for Air Resource Engineering and Science, Clarkson University, Potsdam, NY 13699, USA

[4]Division of Air Resources, New York State Department of Environmental Conservation, Albany, NY 12233, USA

[5]Department of Environmental Medicine, University of Rochester Medical Center, Rochester, NY 14642, USA

* Corresponding author. Tel.: 1-315-268-3861; fax: 1-315-268-4410.

E-mail address: hopkepk@clarkson.edu (P. K. Hopke).

[a] Currently in the Department of Natural Resources and Environmental Sciences, University of Nevada, Reno,1664 N. Virginia Street, Reno, NV, USA

Abstract

In the spring of 2008, a 260 MWe coal-fired power plant (CFPP) located in Rochester, New York was closed over a 4 month period. Using a 2-year data record, the impacts of the shutdown of the CFPP on nearby ambient concentrations of three Hg species were quantified. The arithmetic average ambient concentrations of gaseous elemental mercury (GEM), gaseous oxidized mercury (GOM), and particulate mercury (PBM) during December 2007 to November 2009 were 1.6 ng/m^3, 5.1 pg/m^3, and 8.9 pg/m^3, respectively. The median concentrations of GEM, GOM, and PBM significantly decreased by 12%, 73%, and 50% after the CFPP closed (Mann-Whitney test, $p < 0.001$). Positive Matrix Factorization (EPA PMF v4.1) identified six factors including O_3-rich, traffic, gas phase oxidation, wood combustion, nucleation, and CFPP. When the CFPP was closed, median concentrations of GEM, GOM, and PBM apportioned to the CFPP factor significantly decreased by 25%, 74%, and 67%, respectively, compared to those measured when the CFPP was still in operation (Mann-Whitney test, $p < 0.001$). Conditional probability function (CPF) analysis showed the greatest reduction in all three Hg species was associated with northwesterly winds pointing toward the CFPP. These changes were clearly attributable to the closure of the CFPP.

Keywords

Coal-fired power plant (CFPP), mercury, positive matrix factorization (PMF), conditional probability function (CPF), gas-particle partitioning coefficient

1. Introduction

Mercury (Hg) has been labeled as a Persistent Bioaccumulated Toxic (PBT) chemical by the U.S. EPA since 1997 (U.S. EPA, 1997). Hg is found in various compartments of an ecosystem including sediments where it is often in the form of methylated Hg^{2+} (Engstrom, 2007; Gilmour et al., 1992). There are three operationally defined forms of Hg in the atmosphere, including gaseous elemental mercury (GEM), gaseous oxidized mercury (GOM), and particulate mercury (PBM) (Schroeder and Munthe, 1998). GEM is relative stable with an atmospheric residence time of 0.5 to 2 years because of its low reactivity and limited water solubility (Schroeder and Munthe, 1998). Vegetation uptake, dry deposition, and homogeneous/heterogeneous oxidation reactions are considered as significant sinks of GEM in the atmosphere (Ericksen et al., 2003; Gustin, 2011; Lin et al., 2006; Lin et al., 2007; Schroeder and Munthe, 1998). GOM consists of HgO, HgS, $HgCl_2$, $HgBr_2$, $HgSO_4$, $Hg(OH)_2$, and $Hg(NO_3)_2$ (Feng et al., 2004; Lindberg and Stratton, 1998; Schroeder and Munthe, 1998; Seigneur et al., 1994). GOM and PBM can be rapidly removed by precipitation and dry deposition. Their atmospheric residence times range from days to weeks (Gustin, 2011; Schroeder and Munthe, 1998; Zhang et al., 2009).

Hg is emitted from both natural and anthropogenic sources. The combustion of coal in coal-fired power plants (CFPP) represents the most important anthropogenic source of mercury released to the global atmosphere annually accounting for about 810 Mg/yr, with an important contribution from Asian countries (nearly 50% of the total) (Pirrone et al., 2010). Source profiles including Hg forms, which are necessary to better understand Hg sources are not well documented, in-part because of limited long-term Hg measurements (Gratz and Keeler, 2011; Huang et al., 2010; Keeler et al., 2006; Liu et al., 2007; Lynam and Keeler, 2006). Previously

Positive Matrix Factorization (PMF), Unmix, Quantitative Transport Bias Analysis (QTBA) have been used to identify Hg-related factors that influence Hg wet deposition (Gratz and Keeler, 2011; Keeler et al., 2006). Principle Component Analysis (PCA) also has been applied to explore the variations of atmospheric Hg concentration (Huang et al., 2010; Liu et al., 2007; Lynam and Keeler, 2006). These studies all reported an important coal combustion source that is related to S (or SO_2) and Hg. Results from these studies suggest that coal combustion is a common and significant Hg emission source in the Eastern U.S.

Between January and April 2008, a CFPP located in Rochester, New York was gradually shut down (Wang et al., 2011a). In this study, the impacts of the shutdown of the CFPP on local ambient Hg concentrations were quantified as a part of an extensive project evaluating Rochester air quality using a 2-year data record (Huang et al., 2010, Wang et al., 2011b).

2. Experimental

2.1 Sampling site

Measurements were performed in Rochester, New York, from December 2007 to November 2009. According to 2009 estimates, the population in Rochester is 207,294 (US Census Bureau, http://www.census.gov/), making it the third largest city in New York State. The New York State Department of Environmental Conservation (NYS DEC) maintains a monitoring site in Rochester, NY (43°08’46’’ N, 77°32’54’’ W, Elevation = 137 m, U.S. EPA site code 36-055-1007). This site is northeast and adjacent to the intersection (~ 300 m to the south of the site) of two major highways (I-490 and I-590). The 2005 - 2009 average annual average daily traffic (AADT) counts were 112,291 and 112,549 on I-490 and I-590, respectively. The percentages of

buses and heavy-duty diesel vehicles (HDDV) in the traffic on I-490 and I-590 were 21% and 14%, respectively (Wang et al., 2012).

A coal-fired power plant (estimated emissions ~42 kg-Hg/year) (U.S. EPA, 2010) was located on the shores of Lake Ontario, ~ 12 km north of Rochester downtown area. This CFPP, built in 1948, was one of the state's oldest power plants. It included four coal-fueled power generating units with a total capacity of 260 MWe. A coal-fired steam generator plant (estimated emissions < 5 kg-Hg/year) (U.S. EPA, 2010) at Kodak Park is located in north-central Rochester. Its production and emissions substantially decreased during recent years (Wang et al., 2011b). Huang et al. (2011) and Wang et al. (2011c) reported Hg emissions from winter residential wood combustion, which was mainly located to the south of the monitoring site. Figure 1 shows the locations of the major roadways, the CFPP, the Kodak plant, and the monitoring site in Rochester, NY. The prevailing wind direction was southwesterly. A detailed description of the local meteorology was given by Wang et al. (2011c).

2.2 Instrumentation and data description

A Tekran speciation system (1130/1135/2537A, Tekran Instruments Corp., Ontario, Canada) was used for Hg measurements. An impactor was utilized in the inlet to remove particle larger than 2.5 μm. GOM and PBM were collected on a KCl-coated denuder followed by a quartz filter, respectively, in 2-hour sampling intervals at 10 L/min and sequentially desorbed (1-hour). GEM concentrations were recorded every five minutes during each sampling period. In the desorption cycle, GOM and PBM were desorbed from their collection surface and converted to GEM, and qualified by the analyzer. A detailed description of this system was presented by Landis et al. (2002), Choi et al. (2008), and the standard operation procedure of the Atmospheric

Mercury Network (http://nadp.sws.uiuc.edu/amn/). The detection limit of GOM and PBM (3σ of flush blanks) were 0.46 pg/m^3 and 1.10 pg/m^3, respectively (Huang et al., 2010). The detection limit of GEM reported by the instrument manufacturer is 0.1 ng/m^3 (Tekran®, 2001). The uncertainty of GEM, GOM, and PBM using this method was summarized by Gustin and Jaffe (2010) as ~20%, ~40%, and ~70%, respectively. The GOM concentrations can be influenced by the ambient air ozone concentrations (Lyman et al., 2010). However, this method is still the accepted method for real time atmospheric Hg monitoring.

The number size distribution concentrations of particles with diameter between 10 nm and 500 nm were measured with a time resolution of 5 min using a scanning mobility particle sizer (SMPS), consisting of a differential mobility analyzer (DMA, model 3071, TSI Inc.), a ^{85}Kr aerosol neutralizer (model 3077, TSI Inc.) and a condensation particle counter (CPC, model 3010, TSI Inc.). Data processing, such as inversion of the raw size distributions and multiple charge correction, was performed using the TSI Aerosol Instrument Manager software (AIM, version 8.1). The number concentrations were classified and calculated as a function of three size ranges, 10 to 50 nm, 50 to 100 nm, and 100 to 500 nm.

Continuous mass concentrations of $PM_{2.5}$ were measured using a 50°C tapered element oscillating microbalance (TEOM, R&P 1400a) operated by NYS DEC. The gaseous pollutants (CO, SO_2 and O_3) were continuously measured using standard State and Local Air Monitoring Stations (SLAMS) Federal Reference Method/Federal Equivalent Method (FRM/FEM) gas monitors (Wang et al., 2011b). Measurements of black carbon (BC) concentrations were made using a two-wavelength aethalometer (370 and 880 nm, Model AE-21, Magee Scientific, California, USA) with a time resolution of 5 min. The loading effect on the aethalometer data was corrected using the algorithm developed by Virkkula et al. (2007). Delta-C ($BC_{370\ nm}$ - $BC_{880\ nm}$), which can serve as an indicator of wood combustion particles (Allen et al., 2004; Wang et al., 2011d), was also calculated and included in further data analysis. All instruments aspirated the

ambient air from a height of ~5 m above the ground level. Average number concentrations of 10-50 nm, 50-100 nm and 100-500 nm particles, $PM_{2.5}$ mass concentrations, concentrations of CO, SO_2, O_3, BC, and Delta-C were calculated during every three-hour period to match Hg measurements for further source apportionment modeling.

2.3 Positive matrix factorization (PMF) and conditional probability function (CPF)

PMF is a multivariate factor analysis took that decomposes a matrix of data into two matrices – factor contributions and profiles. It has been comprehensively described by Paatero (1997). EPA PMF v4.1 was used in this study. This method is described in greater detail by Norris et al. (2008, 2010). GEM, GOM, and PBM mass concentrations, number concentrations of 10-50 nm, 50-100 nm and 100-500 nm particles, $PM_{2.5}$ mass concentrations, concentrations of CO, SO_2, O_3, BC and Delta-C were included in the input matrix. The input data matrix includes 4,344 rows and 12 columns. Species measured below detection limits (DL) were replaced by 1/2 DL and assigned an uncertainty equal to 5/6 DL. All missing data were replaced by the geometric mean concentration (Polissar et al., 1998). The data measurement uncertainties and the uncertainties inputted into PMF v4.1 were estimated using the algorithm described by Kasumba et al. (2009). The signal to noise ratios ranged between 2.3 and 7.9 indicating all 12 species were appropriate for modeling.

The sources impacts from various wind directions can be analyzed by CPF. The method description is given by Kim et al (2003). The sources are likely to be located in directions that

have high conditional probability values. In this study, calm wind (wind speed less than 1.0 m/s) were excluded from the analysis because of the isotropic behavior of wind vane under calm winds. Wind sectors of 30° were used starting at 0°. A threshold criterion of the 75th percentile was selected. CFP analysis was performed using the resolved source concentration data (Wang et al., 2011a).

2.4 Gas-particle partitioning coefficient calculation

The gas-particle partitioning coefficient (K_p) of Hg (II) was calculated using the following equation (Rutter and Schauer, 2007a, b):

$$K_p = \frac{PBM/PM_{2.5}}{GOM} \quad (1)$$

where PBM and GOM are PBM and GOM concentrations (pg/m^3), and $PM_{2.5}$ represents fine particle mass concentrations (μg/m^3). The data was filtered by wind direction (between 310° and 330° where the CFPP was located), and were compared between four time periods: December 2007 to April 2008 (CFPP in operation), April 2008 to November 2008, December 2008 to April 2009, April 2009 to November 2009.

3. Results and discussion

3.1 Temporal profiles of Hg

During the entire sampling period, the arithmetic average concentrations of GEM, GOM, and PBM were 1.6 ng/m^3, 5.1 pg/m^3, and 8.9 pg/m^3, respectively, and the median concentrations of GEM, GOM, and PBM were 1.5 ng/m^3, 1.9 pg/m^3, and 5.2 pg/m^3, respectively. The arithmetic

average GEM concentrations during winter 2007 and fall 2009 were slightly higher compared to other periods (Figure 2). The seasonally averaged GOM concentrations ranged from 1.8 to 15.5 pg/m^3. The highest seasonally averaged concentration was observed during spring (March to May), while the lowest was found in winter (December to February). The seasonally averaged PBM concentrations ranged from 3.8 to 28.2 pg/m^3 with the highest in winter and lowest in summer (June to August). Greater PBM concentrations in winter compared to other seasons may have resulted from increased emissions from fuel combustion, particularly wood for space heating (Friedli et al., 2003; Huang et al., 2011), poorer atmospheric mixing conditions, and increased sorption of semivolatile compounds including GOM at lower temperatures (Matsunaga et al., 2003; Rutter and Schauer, 2007a). This seasonal variation is consistent with previous studies (Engle et al., 2010; Huang et al., 2012; Liu et al., 2007, 2010).

The four-boiler CFPP approximately 12 km northwest of the monitoring site was retired during January to April 2008. The first and second boilers closed on 01/31/2008 and 02/14/2008, respectively. The third boiler was shut down on 04/23/2008 and the fourth unit was terminated on 04/01/2008 (Huang et al., 2010). A summary of GEM, GOM, and PBM concentrations measured during December 2007 to April 2008 (CFPP in operation) and during December 2008 to April 2009 (CFPP closure) is presented in Table 1. The ambient median concentrations of GEM, GOM, and PBM in Rochester, NY significantly decreased by 12%, 73%, and 50%, respectively, after the shutdown of the CFPP (Mann-Whitney test, $p < 0.001$).

3.2 Comparison with prior studies

Atmospheric Hg concentrations are substantially elevated in the areas where a CFPP is operating (Table 2). In East St. Louis, IL, the concentrations of all three Hg species were 2-5

magnitudes higher than those measured at a background site (Manolopoulos et al., 2007). Tan et al. (2000) and Feng et al. (2003) reported high Hg concentrations in Guizhou, China due to nearby coal combustion. High GEM concentrations in Taichung, Taiwan were reported to be from ground level point sources, which include a CFPP, a smelter, and some municipal solid waste incinerators (Huang et al., 2012). The Hg concentrations measured in this study were lower than those typically found at other urban locations where the sampling site was in the vicinity of large CFPP. It is probably because the predominant wind direction was southwesterly, which limited the impact of local industrial activities that were located northwest of the sampling site and the annual Hg emission from the CFPP (42 kg/yr ,U.S. EPA, 2010) was distinctly less than those emitted from the other CFPPs investigated in the prior studies.

3.3 PMF results

A range of factor numbers from 4 to 8 was examined. Six factors were identified based on the scaled residuals distributions and the interpretability of the resulting profiles (Wang et al., 2011a). The scaled residuals were approximately symmetrically distributed between -3 and +3. The Q (robust) and Q (true) values were 7,998 and 7,996, respectively. The final FPEAK (rotational parameter) value was 0.05. The six factors were identified as O_3-rich, traffic, gas phase oxidation, wood combustion, nucleation, and the CFPP. The percent contributions of each factor to the measured 12 pollutants are shown in Figure 3. The temporal variations of all six factor contributions are shown in Figure S1. The O_3-rich factor was dominated by O_3 and GEM, while traffic included BC and 100-500 nm particles. A substantial number input of 10-100 nm particles was found in the nucleation factor. Delta-C and PBM are two indictors for wood combustion (Huang et al., 2011; Wang et al., 2011d), and factor 4 contributed 98% and 48%, respectively, of these species. Thus, this factor is classified as wood combustion, which was

dominant in the winter and least important in the summer. Factor 6 contributed 50% PBM and 80% SO_2, respectively, which is defined as the CFPP. The gas phase oxidation factor contributed 85% GOM and 23% O_3, and this factor was primarily found in the summer.

Figure 4 shows the seasonal variations of the CFPP factor contributions to GEM, GOM, and PBM. The factor profiles and contributions were scaled to the measured concentrations of each Hg species. GEM dominated the total Hg concentrations. The December 2008 to April 2009 median GEM, GOM, and PBM concentrations apportioned to the CFPP factor decreased significantly by 25%, 74%, and 67%, respectively compared to those during December 2007 to April 2008 when the CFPP was still in partial operation (Mann-Whitney test, $p < 0.001$). This trend was consistent with the CFPP SO_2 contribution that showed a 64% decrease between 2007 and 2008 (Wang et al., 2011a). These changes were attributed to the shutdown of the CFPP and also reductions in the Kodak industrial activity.

3.4 CPF results

Figure 5 shows the comparison of the directionalities of the CFPP factor contributions to the GEM, GOM, and PBM measured during December 2007 to April 2008 (CFPP in operation) and December 2008 to April 2009 (CFPP closure). In general, the CFPP contributions to the GEM, GOM, and PBM when the wind was from the northwest were greater (but not statistically significant, student's t test, $p > 0.1$) compared to other wind directions. The greatest reduction in the CFPP contributions between the CFPP in operation and the CFPP closure was observed for northwesterly winds, which is consistent with the effects of the closure of the CFPP. After the CFPP was closed, higher contributions of all three Hg species were generally observed when the wind was from the southwest compared to other directions. It appears that CFPPs in western

New York and the Ohio River Valley also influence ambient Hg concentrations in the Upstate New York region (Wang et al., 2011a).

3.5 Gas-particle partitioning coefficient of Hg (II)

Rutter and Schauer (2007a,b) concluded that the gas-particle partitioning coefficient (K_p) of Hg(II) strongly depends on the particle composition and the ambient air temperature. K_p of Hg (II) on ammonium sulfate was reported in the range of 1-10 $m^3/\mu g$ (0.2 $m^3/\mu g$ for filter measurements) (Rutter and Schauer, 2007b). In this study, the arithmetic average K_p of Hg (II) was 1.1 $m^3/\mu g$ and increased to 1.5 $m^3/\mu g$ during December 2008 to April 2009 when the CFPP was already closed (see Table 3). It should be noted that the measurements in this study were done using the Tekran system rather than separate filter samples. The limitations of Tekran instruments were previously reported (Lyman et al., 2010). The arithmetic average K_p of Hg (II) was 67% lower when the CFPP was in operatation than as it was closed probably due to a change of ambient aerosol composition due to the closure of the CFPP.

The linear relationship between K_p and the ambient temperature is summarized in Table 3. The slope during the whole sampling period was -1300 ± 120, which is lower than the number found in North America (Amos et al., 2012). The K_p during these two years was inconstant with the lowest value of -3500 ± 260 during December 2008 - April 2009 and the highest value of -1100 ± 280 during April 2008 and December 2008. The average slopes between April 2008 to December 2008 and April 2009 to December 2009 were substantially different (-1100 vs. -2000), which suggests the impact of other factors on K_p after the CFPP closed.

4. Conclusions

In Rochester, New York, the ambient concentrations of Hg species (especially PBM) were influenced by a local CFPP based on a comparison of results obtained when the CFPP was in operation and after it was closed. Key results are: (1) Statistically significant reductions in the ambient concentrations of GEM, GOM, and PBM were observed. (2) Median GEM, GOM, and PBM concentrations apportioned to the CFPP factor all decreased significantly after the CFPP was closed. (3) The greatest reduction in the CFPP contributions was found for northwesterly winds when the sampling site was downwind of the CFPP. (4) The substantial change of the gas-particle partitioning coefficient of Hg^{2+} was observed.

Acknowledgments

This work was supported by the New York State Energy Research and Development Authority (NYSERDA) through Contracts 8650 and 10604; the United States Environmental Protection Agency (US EPA) through Science to Achieve Results (STAR) grant RD83241501; a Syracuse Center of Excellence Collaborative Activities for Research and Technology Innovation (CARTI) project award, which is supported by a grant from the US EPA (Award No: X-83232501-0); the Electric Power Research Institute underAgreementW06325; the US EPA Atmospheric Clean Air Markets Division and NADP Hg Monitoring Network (EP08H000271). Although the research described in this article has been funded in part by the EPA, it has not been subjected to the Agency's required peer and policy review and, therefore, does not necessarily reflect the views of the Agency and no official endorsement should be inferred. We gratefully acknowledge the substantial assistance from Mr. Dirk Felton and Mr. Tom Everts at NYSDEC.

References

Allen, G., Babich, P., Poirot, R., 2004. Evaluation of a New Approach for Real Time Assessment of Wood Smoke PM. In Air and Waste Management Association Visibility Specialty Conference on Regional and Global Perspectives on Haze: Causes, Consequences and Controversies, Asheville, NC.

Amos, H.M., Jacob, D.J., Holmes, C.D., Fisher, J.A., Wang, Q., Yantosca, R.M., Corbitt, E.S., Galarneau, E., Rutter, A.P., Gustin, M.S., Steffen, A., Schauer, J.J., Graydon, J.A., St. Louis, V.L., Talbot, R.W., Edgerton, E.S., Zhang, Y., Sunderland, E.M., 2012. Gas-particle partitioning of atmospheric Hg (II) and its effect on global mercury deposition. Atmos. Chem. Phys. 12, 591-603.

Choi, H.-D., Holsen, T.M., Hopke, P.K., 2008. Atmospheric Mercury (Hg) in the Adirondacks: Concentrations and Sources. Environ. Sci. Technol. 42, 5644-5653.

Engle, M.A., Tate, M.T., Krabbenhoft, D.P., Schauer, J.J., Kolker, A., Shanley, J.B., H., Bothner,M.H., 2010. Comparison of atmospheric mercury speciation and deposition at nine sites across central and eastern North American. J. Geophys. Res. 115, D18306, 13 PP. doi:10.1029/2010JD014064.

Engstrom, D., 2007. Fish respond when the mercury rises. Proc. Natl. Acad. Sci. 104, 16394 - 16395.

Ericksen, J.A., Gustin, M.S., Schorran, D.E., Johnson, D.W., Lindberg, S.E., Coleman, J.S., 2003. Accumulation of atmospheric mercury in forest foliage. Atmos. Environ. 37, 1613-1622.

Feng, X., Tang, S., Shang, L., Yan, H., Sommar, J., Lindqvist, O., 2003. Total gaseous mercury in the atmosphere of Guiyang, PR China. Sci. Total Environ. 304, 61-72.

Feng, X., Lu, J.Y., Grégoire, C., Hao, Y., Banic, C.M., Schroeder, W., 2004. Analysis of inorganic mercury species associated with airborne particulate matter/aerosols: method development. Anal. Bioanal. Chem. 380, 683–689.

Friedli, H. R., Radke, L. F., Lu, J. Y., Banic, C. M., Leaitch, W. R., MacPherson, J. I., 2003. Mercury emissions from burning of biomass from temperate North American forests: laboratory and airborne measurements. Atmos. Environ. 37 (2), 253–267.

Gilmour, C.C., Henry, E.A., Mitchell, R., 1992. Sulfate stimulation of mercury methylation in freshwater sediments. Environ. Sci. Technol. 26, 2281-2287.

Gratz, L.E., Keeler, G.J., 2011. Sources of mercury in precipitation to Underhill, VT. Atmos. Environ. 45, 5440-5449.

Gustin, M.S., 2011. Exchange of Mercury between the Atmosphere and Terrestrial Ecosystems. in: Liu, G., Cai, Y., O'Driscoll, N. (Eds.), Advances in Environmental Chemistry and Toxicology of Mercury. John Wiley and Sons.

Huang, J., Choi, H.-D., Hopke, P.K., Holsen, T.M., 2010. Ambient Mercury Sources in Rochester, NY: Results from Principle Components Analysis (PCA) of Mercury Monitoring Network Data. Environ. Sci. Technol. 44, 8441-8445.

Huang, J., Hopke, P. K., Choi, H.-D., Laing, J. R., Cui, H., Zananski, T. J., Chandrasekaran, S. R., Rattigan, O. V., Holsen, T. M., 2011. Mercury (Hg) emissions from domestic biomass combustion for space heating. Chemosphere 84 (11), 1694-1699.

Huang, J., Liu, C.-K., Huang, C.-S., Fang, G.-C., 2012. Atmospheric mercury pollution at an urban site in central Taiwan: Mercury emission sources at ground level. Chemosphere 87 (5), 579-585.

Kasumba, J., Hopke, P. K., Chalupa, D. C., and Utell, M.J., 2009. Comparison of Sources of Submicron Particle Number Concentrations Measured at Two Sites in Rochester, NY. Sci. Total Environ. 407, 5071–5084.

Keeler, G.J., Landis, M.S., Norris, G.A., Christianson, E.M., Dvonch, J.T., 2006. Sources of mercury wet deposition in eastern Ohio, USA. Environ. Sci. Technol. 40, 5874-5881.

Kim, E., Hopke, P.K., Edgerton, E.S., 2003. Source identification of Atlanta aerosol by positive matrix factorization. J. Air Waste Manag. Assoc. 53, 731-739.

Landis, M.S., Stevens, R.K., Schaedlich, F., Prestbo, E.M., 2002. Development and characterization of an annular denuder methodology for the measurement of divalent inorganic reactive gaseous mercury in ambient air. Environ. Sci. Technol. 36, 3000-3009.

Lin, C.-J., Pongprueksa, P., Lindberg, S.E., Pehkonen, S.O., Byun, D., Jang, C., 2006. Scientific uncertainties in atmospheric mercury models I: Model science evaluation. Atmos. Environ. 40, 2911-2928.

Lin, C.-J., Pongprueksa, P., Russell Bullock Jr, O., Lindberg, S.E., Pehkonen, S.O., Jang, C., Braverman, T., Ho, T.C., 2007. Scientific uncertainties in atmospheric mercury models II: Sensitivity analysis in the CONUS domain. Atmos. Environ. 41, 6544-6560.

Lindberg, S.E., Stratton, W.J., 1998. Atmospheric mercury speciation: concentrations and behavior of reactive gaseous mercury in ambient air. Environ. Sci. Technol. 32, 49-57.

Liu, B., Keeler, G.J., Dvonch, J.T., Barres, J.A., Lynam, M.M., Marsik, F.J., Morgan, J.T., 2007. Temporal variability of mercury speciation in urban air. Atmos. Environ. 41, 1911-1923.

Liu, B., Keeler, G. J., Dvonch, J. T., Barres, J. A., Lynam, M. M., Marsik, F. J., Morgan, J. T., 2010. Urban-rural differences in atmospheric mercury speciation. Atmos. Environ. 44, 2013-2023.

Lynam, M.M., Keeler, G.J., 2006. Source-receptor relationships for atmospheric mercury in urban Detroit, Michigan. Atmos. Environ. 40, 3144-3155.

Lyman, S. N.; Jaffe, D. A.; Gustin, M. S., 2010. Release of mercury halides from KCl denuders in the presence of ozone. Atmos. Chem. Phys. 10, 8197-8204.

Manolopoulos, H., Snyder, D.C., Schauer, J.J., Hill, J.S., Turner, J.R., Olson, M.L., Krabbenhoft, D.P., 2007. Sources of speciated atmospheric mercury at a residential neighborhood impacted by industrial sources. Environ. Sci. Technol. 41, 5626-5633.

Matsunaga, S., Mochida, M., Kawamura, K., 2003. Growth of organic aerosols by biogenic semi-volatile carbonyls in the forestall atmosphere. Atmos. Environ. 37 (15), 2045-2050.

Norris, G.,Vedantham, R.,Wade, K., Brown, S., Prouty, J., Foley, C., 2008. EPA positive matrix factorization (PMF) 3.0 fundamentals & user guide. U.S. Environmental Protection Agency, Office of Research and Development, Washington, DC.

Norris, G., Vedantham, R., Duvall, R., Wade, K., Brown, S., Prouty, J., Bai, S., DeWinter, J., Foley, C., 2010. EPA positive matrix factorization (PMF) 4.1 fundamentals and user guide. Draft version. U.S. Environmental Protection Agency, Office of Research and Development, Washington, DC.

Paatero, P., 1997. Least squares formulation of robust non-negative factor analysis. Chemometr. Intell. Lab. 37:23-35.

Pirrone, N., Cinnirella, S., Feng, X., Finkelman, R.B., Friedli, H.R., Leaner, J., Mason, R., Mukherjee, A.B., Stracher, G., Streets, D.G., Telmer, K., 2010. Global mercury emissions to the atmosphere from anthropogenic and natural sources. ATMOS. CHEM. PHYS., 10, 5951–5964.

Polissar, A. V., Hopke, P.K., Paatero, P., 1998. Atmospheric aerosol over Alaska 2. Elemental composition and sources. J. Geophys. Res. 103 (D15), 19045-19057. doi:10.1029/98JD01212.

Rutter, A.P., Schauer, J.J., 2007a. The effect of temperature on the gas-article partitioning of reactive mercury in atmospheric aerosols. Atmos. Environ. 41, 8647-8657.

Rutter, A.P., Schauer, J.J., 2007b. The impact of aerosol composition on the particle to gas partitioning of reactive mercury. Environ. Sci. Technol. 41, 3934-3939.

Schroeder, W.H., Munthe, J., 1998. Atmospheric mercury--An overview. Atmos. Environ. 32, 809-822.

Seigneur, C., Wrobel, J., Constantinou, E., 1994. A chemical kinetic mechanism for atmospheric inorganic mercury. Environ. Sci. Technol. 28, 1589-1597.

Tan, H., He, J.L., Liang, L., Lazoff, S., Sommer, J., Xiao, Z.F., Lindqvist, O., 2000. Atmospheric mercury deposition in Guizhou, China. Sci. Total Environ. 259, 223-230.

U.S. EPA, 1997. Mercury study report to congress. Office of Air Quality Planning and Standards and Office of Research and Development.

U.S. EPA, 2010. Document for the Final 2005 Point Source National Emission Inventory. US Environmental Protection Agency, Research Triangle Park, NC. http://www.epa.gov/ttn/chief/net/2005inventory.html.

Tekran, Model 2537 Mercury Vapor Analyzer User Manual. Tekran Inc.: Toronto, Ontario, 2001.

Virkkula, A., MäKelä, T., Hillamo, R., Yli-Tuomi, T., Hirsikko, A., Hämeri, K., Koponen, I., 2007. A simple procedure for correcting loading effects of aethalometer data. J. Air Waste Manag. Assoc. 57, 1214-1222.

Wang, Y., Hopke, P. K., Chalupa, D. C., Utell, M. J., 2011a. Effect of the shutdown of a coal-fired power plant on urban ultrafine particles and other pollutants. Aerosol Sci. Technol. 45 (10), 1245-1249.

Wang, Y., Hopke, P. K., Chalupa, D. C., Utell, M. J., 2011b. Long-term study of urban ultrafine particles and other pollutants. Atmos. Environ. 45, 7672-7680.

Wang, Y., Hopke, P.K., Rattigan, O.V., Zhu, Y., 2011c. Characterization of ambient black carbon and wood burning particles in two urban areas. J. Environ. Monit. 13, 1919-1926.

Wang, Y., Hopke, P. K., Rattigan, O. V., Xia, X., 2011d. Characterization of residential wood combustion particles using the two-wavelength aethalometer. Environ. Sci. Technol. 45 (17), 7387-7393.

Wang, Y., Hopke, P.K., Rattigan, O.V., Chalupa, D.C., Utell, M.J., 2012. Multiple year black carbon measurement and source apportionment using Delta-C in Rochester, NY. J. Air Waste Manag. Assoc. 62 (8), 880-887.

Zhang, L., Wright, L.P., Blanchard, P., 2009. A review of current knowledge concerning dry deposition of atmospheric mercury. Atmos. Environ. 43, 5853-5864.

Table 1

Summary of GEM, GOM, and PBM concentrations.

Species		Period	
		12/2007 – 04/2008 (CFPP in operation)	12/2008 – 04/2009 (CFPP closure)
GEM (ng/m^3)	Arithmetic average (1SD*)	1.8 (0.3)	1.5 (0.2)
	Median	1.7	1.5
GOM (pg/m^3)	Arithmetic average (1SD)	9.9 (17.0)	3.9 (7.7)
	Median	5.1	1.4
PBM (pg/m^3)	Arithmetic average (1SD)	21.8 (24.0)	9.2 (7.3)
	Median	14.5	7.3

**SD: Standard deviation*

Table 2
Summary of atmospheric Hg concentrations (presented in range or arithmetic average ± 1SD) in the nearby area of CFPP.

Location	Description	GEM (ng/m^3)	GOM (pg/m^3)	PBM (pg/m^3)	Reference
East St. Louis, IL	6 CFPP with numerous other point sources within 100 km	50-200	5,000-35,000		Manolopoulos et al., 2007
Guizhou, China	--	7.39	--	--	Tan et al., 2000
Guiyang, China	1 CFPP and 1 cement plant within 20 km	9.0 ± 4.2	800 ± 40		Feng et al., 2003
Taichung, Taiwan	1 CFPP with numerous other point sources within 50 km	6.1 ± 3.9	330 ± 150	71 ± 46	Huang et al., 2012
Puerto, Rice	Background site	1.4 ± 0.1	1.5 ± 1.6	1.2 ± 1.4	Engle et al., 2010
Rochester, NY	1 CFPP within 15 km	1.6 ± 0.3	5.1 ± 10.2	8.9 ± 13.5	This study

Table 3
Summary of the K_p of Hg (II). The slope and intercept represent the constant in the equation of $Log(K_p^{-1})$ = slope × 1/T + intercept.

Time period	**slope**	**intercept**	**r^2**	**K_p ($m^3/\mu g$)**
Overall	-1300 ± 120	5.0 ± 0.4	0.11, $p < 0.01$	1.1 ± 4.0
December 2007 – April 2008	-1400 ± 330	5.7 ± 1.2	0.09, $p < 0.01$	0.5 ± 0.5
December 2008 – April 2009	-3500 ± 260	13 ± 1.0	0.35, $p < 0.01$	1.5 ± 6.7
April 2008 – December 2008	-1100 ± 280	4.3 ± 1.0	0.06, $p < 0.01$	1.2 ± 1.3
April 2009 – December 2009	-2000 ± 490	7.4 ± 1.7	0.07, $p < 0.01$	1.2 ± 4.0

Fig. 1. Map of the locations of the sampling site, the major roadways, and the Hg emission sources in Rochester, New York.

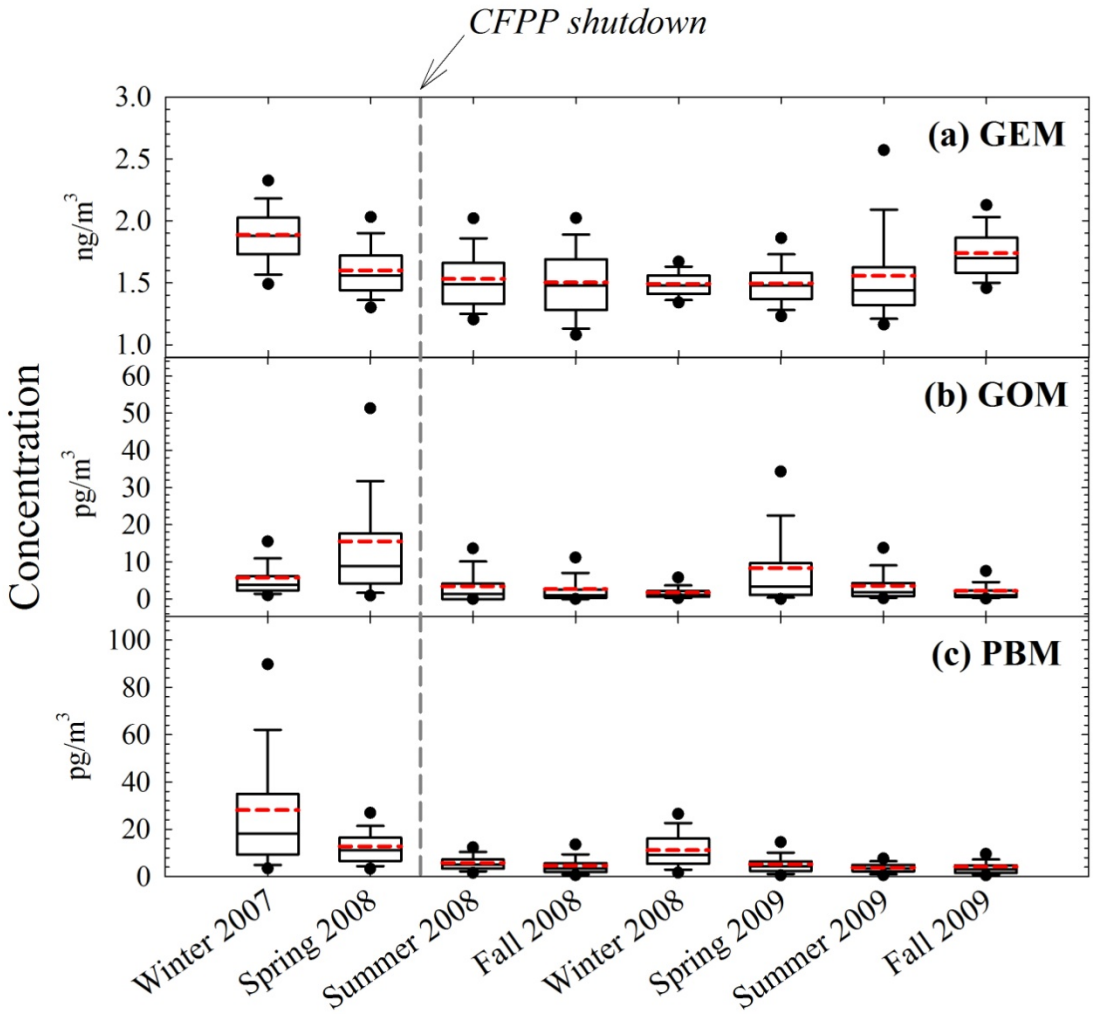

Fig. 2. Seasonal variation of GEM (ng/m^3), GOM (pg/m^3), and PBM (pg/m^3) in Rochester, NY, during the sampling period starting from December 2007 to November 2009. The upper and lower boundaries of the box indicate the 75th and 25th percentiles. The whiskers above and below the box show the 90th and 10th percentiles. The dots above and below the box represent the 95th and 5th percentiles. The red dash line represents the arithmetic average value. Spring (March-May), summer (Jun-Aug), fall (Sep-Nov), winter (Dec-Feb).

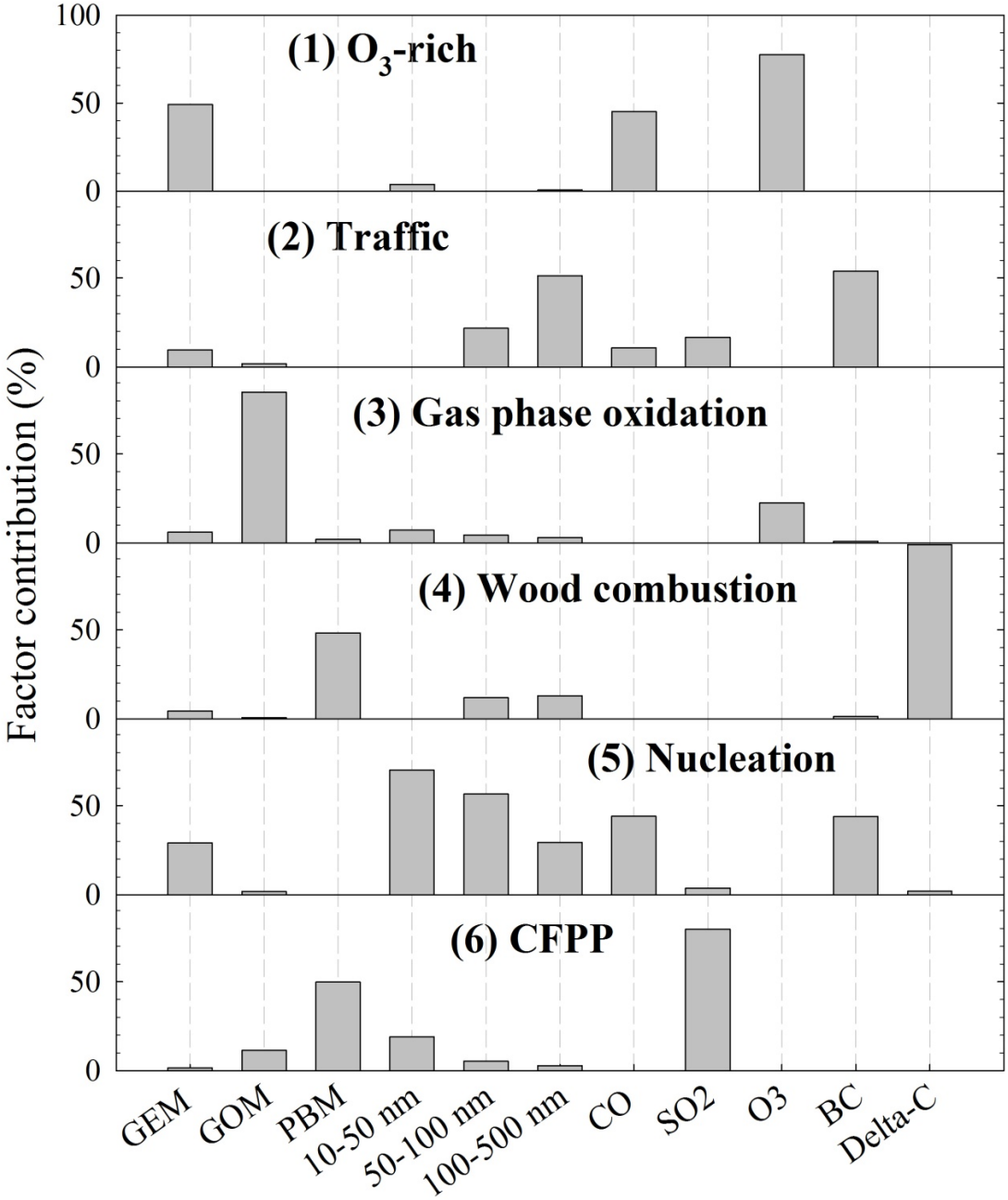

Fig. 3. The contribution percentage of each factor to the pollutants concentrations.

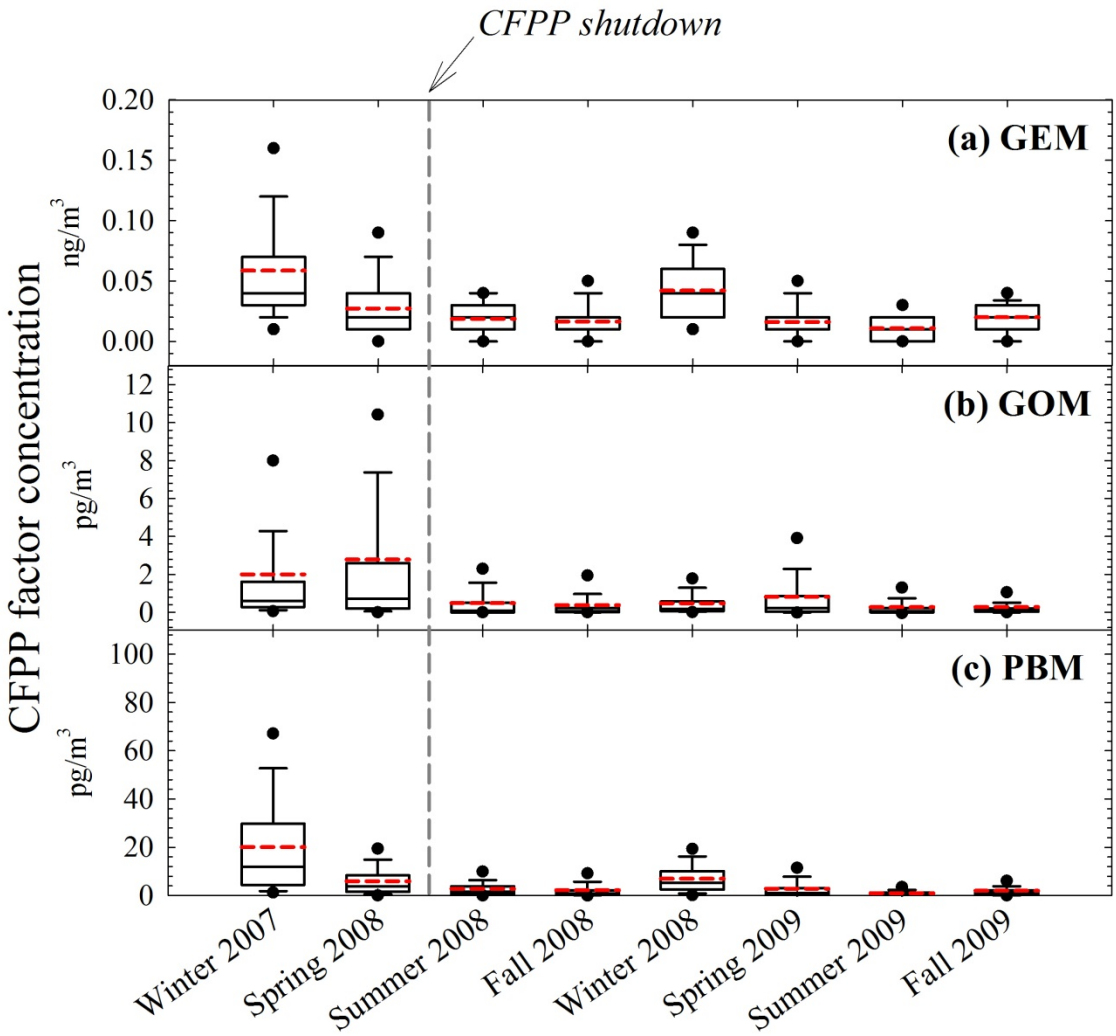

Fig. 4. Seasonal variations of contributions of the CFPP factor to GEM, GOM, and PBM. The upper and lower boundaries of the box indicate the 75th and 25th percentiles. The whiskers above and below the box show the 90th and 10th percentiles. The dots above and below the box represent the 95th and 5th percentiles. The red dash line represents the arithmetic mean value. Spring (March-May), summer (Jun-Aug), fall (Sep-Nov), winter (Dec-Feb).

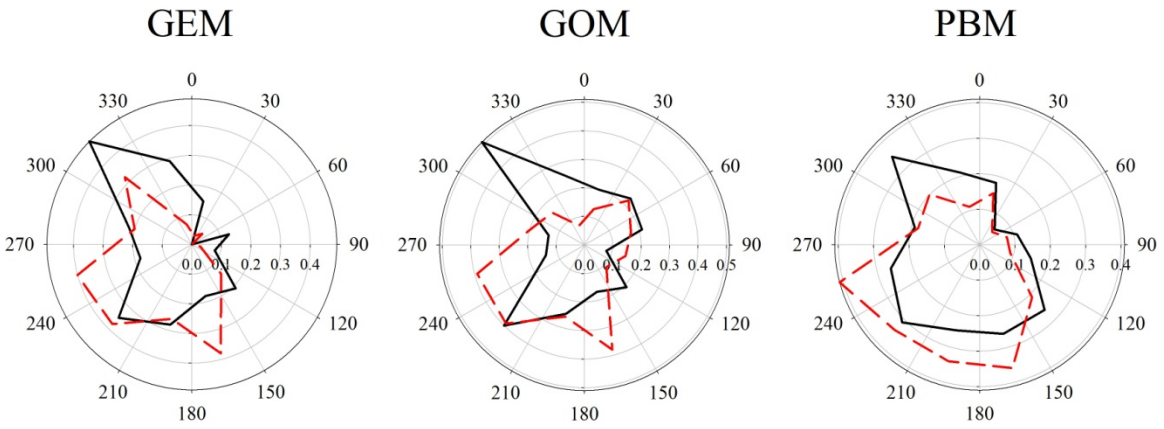

Fig. 5. Comparison of the directionalities of the CFPP factor contributions to the GEM, GOM, and PBM. The black solid line represents December 2007 to April 2008 data (CFPP in operation). The red dash line represents December 2008 to April 2009 data (CFPP closure).

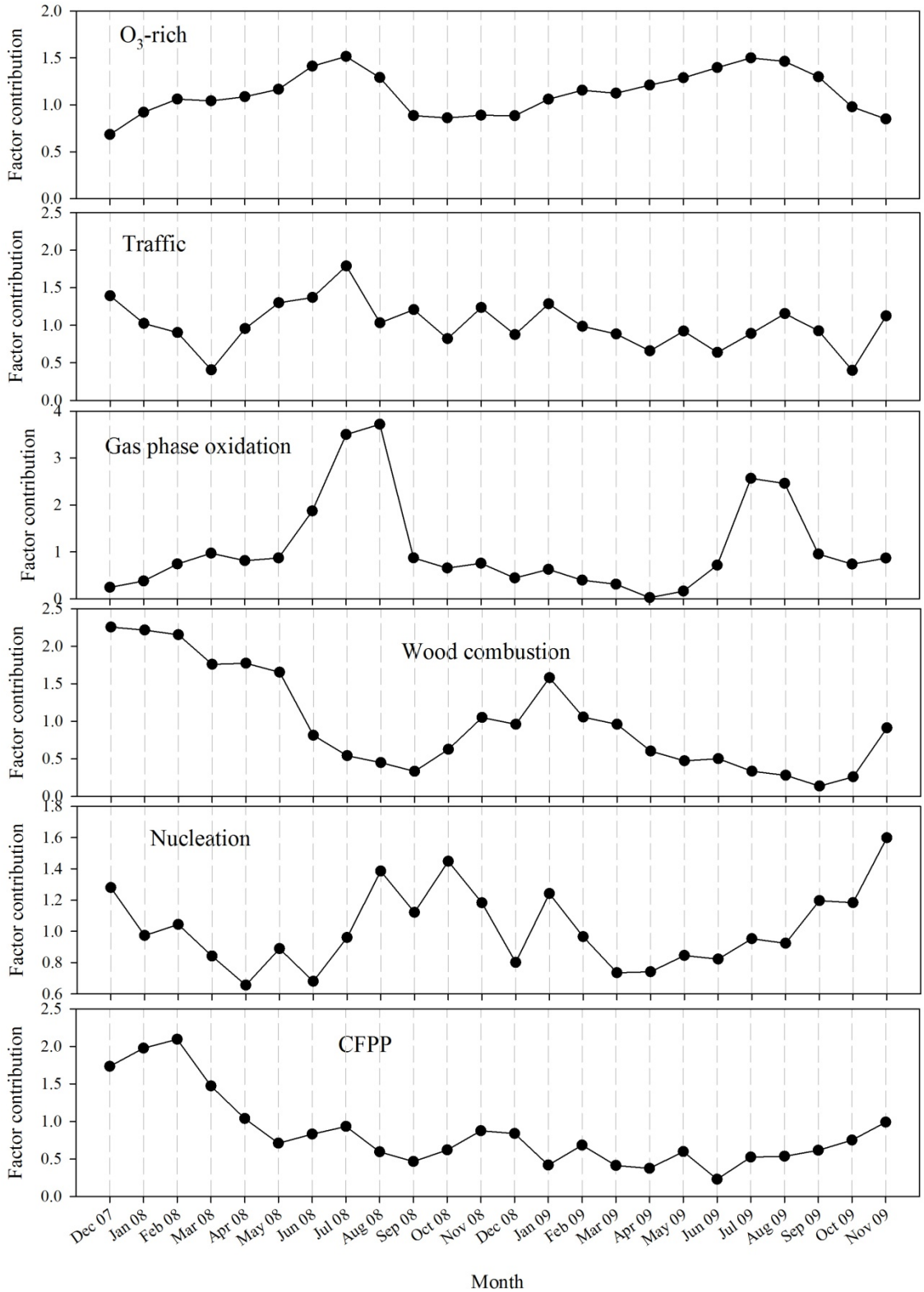
O3-rich
Traffic
Gas phase oxidation
Wood combustion
Nucleation
CFPP
Factor contribution
Dec 07
Jan 08
Feb 08
Mar 08
Apr 08
May 08
Jun 08
Jul 08
Aug 08
Sep 08
Oct 08
Nov 08
Dec 08
Jan 09
Feb 09
Mar 09
Apr 09
May 09
Jun 09
Jul 09
Aug 09
Sep 09
Oct 09
Nov 09
Month

Fig. S1. Temporal variations of all six factor contributions.